2013 European Control Conference (ECC)
July 17-19, 2013, Zürich, Switzerland.

Smooth Frequency Domain Parametric Optimization in Loop-Shaping Control

Erkki Lantto, Vesa Hölttä, Kai Zenger, Ville Tommila

Abstract—**This paper presents two tools for frequency domain parametric optimization. The first tool is an approximation of the square of the largest singular value. This approximation works for complex matrices and enables using smooth constrained optimization methods, like sequential quadratic programming, in the multi-input-multi-output control system design. The second tool is a cost effective controller parametrization, which is based on the Hilbert transform. We also give a simple example to help the reader to get started with this synthesis framework.**

I. Introduction

THE tools and methods presented in this paper have been originally developed to meet the practical challenges in control of active magnetic bearings (AMB) in industrial high speed machines [19]. A good introduction to AMB in general and to the control of AMB is found in [23]. During the years, numerous approaches have been used for AMB controller synthesis [23]. Of all those methods, mu-synthesis has been probably the most potential general purpose approach. As demonstrated in [9], many characteristics of AMB control, like compliance specification, unmodeled high frequency dynamics, and gain variations are properly treated in the mu-framework. However, incorporating rotational speed as a real and repeated uncertainty correctly into the synthesis procedure seems to be challenging [24]. In addition, real world synthesis tasks sometimes include special requirements, like restrictions in controller structure, requirement of a stable controller, need to levitate a slightly modified rotor during service, for instance. Also, utilization of measured frequency response data effectively in the synthesis procedure is a nontrivial problem. Such needs are difficult to deal with using traditional synthesis methods. Therefore, parametric optimization was adopted.

Parametric optimization has been used already for a long time to design controllers. In [25] time domain specifications were formulated to a set of inequalities, and a moving boundaries algorithm was used to find a feasible solution. An automatic loop shaping approach for quantitative feedback theory [14] (QFT) framework was proposed in [11]. In [7] a similar method was proposed, and linear programming was used in the search of optimum. Successive quadratic programming (SQP) was used in [10] to optimize a controller subject to multiple frequency domain specifications. In [15] the H-infinity norm was minimized in a multimodel problem setup. The authors parametrized the controller using rational transfer functions and formulated the synthesis task into a convex optimization problem using a desired open loop transfer function. In [2] a bundling method was presented to minimize H-infinity norm in multimodel multi-input-multi-output (MIMO) systems under controller structure constraints. In [3] the method was extended for structured singular value minimization. In [2] and [3] the largest singular value (LSV) of some frequency response matrix is minimized over a frequency range. The fundamental difficulty in optimizing the LSV using parametric optimization is that the LSV is not differentiable when two largest singular values coincide [16], which leads to a nonsmooth optimization problem. Convergence of nonsmooth methods may be slow near the local optimum, as noted in [2]. Our first contribution is an approximation for the square of LSV. This upper bound is twice continuously differentiable and has guaranteed tolerance. Therefore, it enables using smooth constrained optimization algorithms, like SQP, in MIMO synthesis. Many smooth optimization methods can guarantee fast local convergence [21].

Our second contribution is a new method for controller parametrization. Even though parametric optimization has been studied a lot, the parametrization itself has not got much attention. Most of the papers concentrate on optimizing the coefficients of a simple controller, like PID. In case of AMB, simple PID is rarely sufficient to obtain satisfactory results. The challenge is to parametrize a high order controller cost effectively so that numerical problems are avoided, and solution time remains in so short level that the algorithm can be considered as an interactive tool. Laguerre basis, used for example in [15], is an option especially when the resulting controller behaves relatively smoothly in the frequency domain. However, when rapid maneuvers are expected in some parts of the frequency domain, Laguerre basis is not so effective anymore. It does

Manuscript received October 26, 2012.

Erkki Lantto is with Sulzer Pump Solutions Finland Oy, Espoo, Finland (phone: +358405017130; fax:+358207618580; e-mail: erkki.lantto@sulzer.com)

Vesa Hölttä is with Sulzer Pump Solutions Finland Oy (e-mail: vesa.holtta@sulzer.com).

Kai Zenger is with Aalto University, School of Electrical Engineering, Espoo, Finland (e-mail: kai.zenger@aalto.fi).

Ville Tommila is with Sulzer Pump Solutions Finland Oy (e-mail: ville.tommila@sulzer.com).

not enable concentrating the design freedom to important frequency regions, which leads to uneconomic parametrization when measured as a number of decision variables and constraints. A better solution in this respect can be obtained with the parametrization in [1], but translating the information of the specifications and templates to suitable pole clusters is a nontrivial problem. In [11] and [7] the controller was parameterized by giving a piecewise linear controller amplitude curve in a frequency grid, and using Bode's gain-phase relations [6] to obtain the phase curve. This approach is tempting because it enables effective adjustment of design freedom, simply by adjusting the density of the grid points in the frequency axis. This is almost what is needed, but for the present class of processes the inherent limitation to minimum phase controllers is a serious drawback in parametrizing the amplitude-phase curve. According to our experience, the AMB controllers tend to be non-minimum phase. In our parametrization the real or imaginary part of the controller is defined in a finite frequency grid and the other part is obtained by Hilbert transform. This parametrization allows non-minimum phase controllers as well. Even though the relations between the real and imaginary parts and analytic solutions for Hilbert transforms of piecewise polynomials have been known for a long time ([6], [13]) the authors are not aware that such parametrization would have been used in control system synthesis.

This paper is organized as follows. The LSV approximation is presented in Section 2 and the parametrization in Section 3. In Section 4 we give a simple example and the conclusions are given in Section 5.

II. SMOOTH APPROXIMATION OF LSV

Let us consider the matrix $\boldsymbol{Q}(\boldsymbol{x})\in\mathbb{C}^{M\times P}$, which depends on the real parameter vector $\boldsymbol{x}=[x_1\ x_2\ \ldots\ x_L]^T\in\mathbb{R}^L$. We assume that $\boldsymbol{Q}$ is twice continuously differentiable with respect to $\boldsymbol{x}$. Let us denote the LSV of $\boldsymbol{Q}$ by $\bar{\sigma}(\boldsymbol{Q})$. In the following, we present a smooth approximation for the square of the LSV, $\bar{\sigma}^2(\boldsymbol{Q})$.

Let $\boldsymbol{Z}=\boldsymbol{Q}^H\boldsymbol{Q}$, when P≤M and $\boldsymbol{Z}=\boldsymbol{Q}\boldsymbol{Q}^H$ otherwise. The eigenvalues of $\boldsymbol{Z}$ are the squares of the singular values of $\boldsymbol{Q}$. The characteristic polynomial of $\boldsymbol{Z}$ is of the form

$$\begin{aligned} P(r,\boldsymbol{x}) &= \det\left(r\boldsymbol{I}-\boldsymbol{Z}(\boldsymbol{x})\right) \\ &= r^N + a_{N-1}(\boldsymbol{x})r^{N-1} + \ldots + a_0(\boldsymbol{x}), \end{aligned} \tag{1}$$

where N=max(P,M) and $\boldsymbol{I}$ denotes unity matrix. The coefficients of the characteristic polynomial are real because $\boldsymbol{Z}$ is Hermitian, and twice continuously differentiable. All roots of $P(r,\cdot)$ are real and nonnegative. The largest root is $\bar{\sigma}^2$. Let us define the modified polynomial, P_ε, as follows

$$P_\varepsilon(r,\boldsymbol{x}) = P(r,\boldsymbol{x}) - \varepsilon^N \tag{2}$$

where ε is an arbitrary tolerance, $\varepsilon\in\mathbb{R}$, ε >0. Let us denote the real roots of P_ε as $p_n(\boldsymbol{Q})$ and number them in descending order ($p_1>p_2,\ldots$). Since $P_\varepsilon(\bar{\sigma}^2,x)=-\varepsilon^N$ and $\lim_{r\to\infty} P_\varepsilon(r,:)=\infty$, it is clear that P_ε has at least one real root $>\bar{\sigma}^2$. Our approximation of the square of LSV is the largest of those roots (p_1) and we denote it by $\eta(\boldsymbol{Q})$. In the following we prove that this approximation is twice continuously differentiable with respect to $\boldsymbol{x}$ and fulfills

$$\bar{\sigma}^2(\boldsymbol{Q}) < \eta(\boldsymbol{Q}) \le \bar{\sigma}^2(\boldsymbol{Q}) + \varepsilon. \tag{3}$$

Write the characteristic polynomial in the form

$$P(r,\cdot) = \prod_{i=1}^{N}\left(r-\sigma_i^2\right) \tag{4}$$

where σ_i are the singular values of $\boldsymbol{Q}$. For $r>\bar{\sigma}^2$

$$P(r,\cdot) = \left(r-\bar{\sigma}^2\right)^N \prod_{i=1}^{N}\frac{\left(r-\sigma_i^2\right)}{\left(r-\bar{\sigma}^2\right)} \ge \left(r-\bar{\sigma}^2\right)^N. \tag{5}$$

Thus, P_ε cannot have real roots $>\bar{\sigma}^2+\varepsilon$. See also Fig. 1. Therefore, (3) must hold. From (4) it is seen that $\partial P/\partial r>0$ for $r>\bar{\sigma}^2$, which means that P_ε has exactly one real root for $r>\bar{\sigma}^2$ and this root is simple. To prove differentiability of η, we differentiate the equation $P_\varepsilon(\eta, \boldsymbol{x})=0$ with respect to x_i and obtain

$$\frac{\partial P}{\partial \eta}\frac{\partial \eta}{\partial x_i} + \frac{\partial P}{\partial x_i} = 0 \tag{6}$$

Evaluation of $\partial P/\partial\eta$ is trivial and expression for $\partial P/\partial x_i$ is obtained applying the following fact [22]

$$\frac{\partial \det(\boldsymbol{Y})}{\partial x} = \det(\boldsymbol{Y})\,\mathrm{Trace}\left(\boldsymbol{Y}^{-1}\frac{\partial \boldsymbol{Y}}{\partial x}\right) \tag{7}$$

to matrix $\boldsymbol{Y}=\eta\boldsymbol{I}-\boldsymbol{Z}$. So, the partial derivative is

$$\frac{\partial \eta}{\partial x_i} = -\varepsilon^N\,\mathrm{Trace}\left(\left(\eta\boldsymbol{I}-\boldsymbol{Z}(\boldsymbol{x})\right)^{-1}\frac{\partial \boldsymbol{Z}}{\partial x_i}\right) \Big/ \frac{\partial P}{\partial r} \tag{8}$$

As mentioned earlier, $\partial P/\partial r>0$. Matrix $\eta\boldsymbol{I}-\boldsymbol{Z}$ is invertible,

because $\eta > \bar{\sigma}^2$. Thus, η is at least once continuously differentiable with respect to $\boldsymbol{x}$. By differentiating (6) with respect to x_j the elements of the Hessian can be obtained and it is seen that η is twice continuously differentiable.

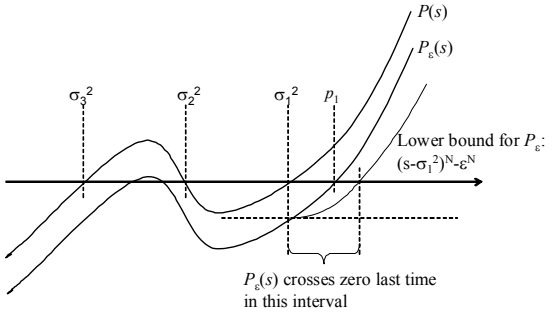

Fig. 1. Behaviour of P and P_ε.

III. PARAMETRIZATION

In this section a method of parametrizing a set of stable SISO transfer functions is presented.

It is a well known fact that the real and imaginary parts of a stable transfer function are tightly related [6] and that the relation is given by the Hilbert transform [13]. The Hilbert transform, v, of function u is defined as follows [4]:

$$v(x) = \frac{1}{\pi} \mathrm{P} \int_{-\infty}^{\infty} \frac{u(x')}{x' - x} dx', \tag{9}$$

where P stands for Cauchy Principal value. Consider function $f(s)$, which is analytic in the right half plane (RHP). Take point ix on the imaginary axis. If $u(x)=\mathrm{Re}(f(\mathrm{i}x))$ then $\mathrm{Im}(f(\mathrm{i}x))=v(x)+c$, where c is a constant. On the other hand, if $u(x)=\mathrm{Im}(f(\mathrm{i}x))$ then $\mathrm{Re}(f(\mathrm{i}x))=-v(x)+c$. This leads to the idea of parametrizing the controller by defining either the real or the imaginary part of the frequency response curve and obtaining the other part using the Hilbert transform. In [13] the Hilbert transform has been derived for continuous piecewise linear functions and also for functions that have a continuous and piecewise linear first derivative. We use a similar approach in our parametrization. Conjugate symmetry of the frequency response function can be assumed and utilized in the derivation of the relations [6]. We do not want to assume this because the capability of dealing with non conjugate symmetric frequency responses is a valuable feature especially in the AMB process.

To define a parametrized set of functions $\{u_S(x)\}$ we select a monotonously increasing grid of points $\{x_{S1},...,x_{SN}\}$ and smoothing parameters $\{w_{S1},...,w_{SN}\}$. These 2N real numbers define a set of piecewise linear smoothed functions, u_S, which are zero in infinity, see Fig. 2.

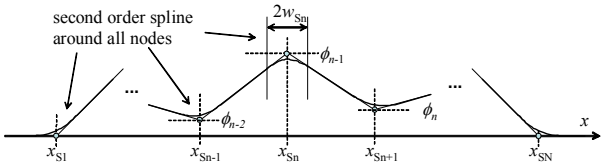

Fig. 2. Form of the u_S-finction.

Function u_S can be expressed in the form

$$u_S(x) = \sum_{n=1}^{N-2} \phi_n u_{ST}(x, x_{Sn}, x_{Sn+1}, x_{Sn+2}, w_{Sn}, w_{Sn+1}, w_{Sn+2}), \tag{10}$$

where $u_{ST}(x,x_L,x_T,x_R,w_L,w_T,w_R)$ is a smoothed triangle function, defined in Fig. 3 and parameters ϕ_n are real. Second order spline curves are introduced to obtain a continuous first derivative. They are not crucial for the method, but with them infinite derivatives are avoided in the Hilbert transform of u_{ST}.

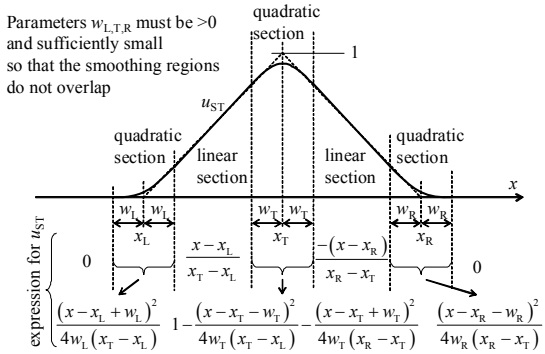

Fig. 3. Smoothed triangle function $u_{ST}(x,x_L,x_T,x_R,w_L,w_T,w_R)$.

The Hilbert transform of u_S is of the form

$$v_S(x) = \sum_{n=1}^{N-2} \phi_n v_{ST}(x, x_{Sn}, x_{Sn+1}, x_{Sn+2}, w_{Sn}, w_{Sn+1}, w_{Sn+2}), \tag{11}$$

where v_{ST} is the Hilbert transform of the smoothed triangle function u_{ST}. Following [13] it is straightforward to verify that

$$v_{ST}(x, x_L, x_T, x_R, w_L, w_T, w_R) = \frac{(x_R - x_L) q(x - x_T, w_T)}{\pi (x_T - x_L)(x_R - x_T)} - \frac{q(x - x_L, w_L)}{\pi (x_T - x_L)} - \frac{q(x - x_R, w_R)}{\pi (x_R - x_T)} \tag{12}$$

where q is a real valued function of two real arguments:

$$q(x, w) = \frac{1}{4w}\left[(x+w)^2 \ln|x+w| - (x-w)^2 \ln|x-w| \right], \tag{13}$$

where ln stands for the natural logarithm. It is also

straightforward to prove that v_{ST} is continuous, has a continuous first derivative and $xv_{ST}(x,\cdot)$ approaches a nonzero constant for large x. Examples of u_{ST} and v_{ST} are shown in Fig. 4.

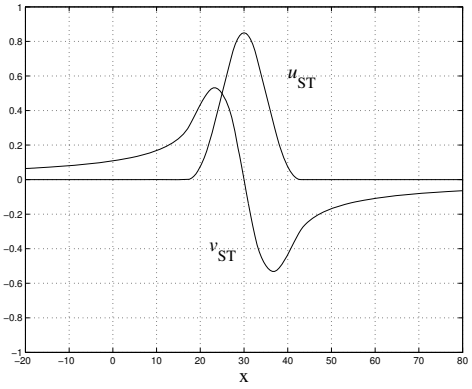

Fig. 4. Smoothed triangle function $u_{ST}(x,20,30,40,3,3,3)$ and its Hilbert transform $v_{ST}(x,20,30,40,3,3,3)$.

Corresponding to every parameter vector value there is a unique pair, $u_S(x)$ and $v_S(x)$, which define values of some function of complex variable $H_S(s)$ on the imaginary axis as $H_S(ix)=u_S(x)+iv_S(x)$ or $H_S(ix)=-v_S(x)+iu_S(x)$. From above it is clear that H_S is linear in respect to variables ϕ_n. For example, in the former case

$$H_S(s)=\sum_{n=1}^{N}\phi_n H_{ST}\left(s,x_{Sn},x_{Sn+1},x_{Sn+2},w_{Sn},w_{Sn+1},w_{Sn+2}\right) \quad (14)$$

where $H_{ST}(s,:)$ is a function analytic in the RHP and which real and imaginary parts in the imaginary axis point ix are $u_{ST}(x,:)$ and $v_{ST}(x,:)$, respectively. Values of $H_S(s)$ in RHP can be evaluated using Cauchy integral formula [4]. By straightforward inspection it is verified that $H_S(s)$ obtained using Cauchy integral formula is indeed analytic in the RHP, vanish at infinity and in the imaginary axis equals the values defined by u_S and v_S. Function $H_S(s)$ is not a rational transfer function but using Runge's theorem [12] it is straightforward to prove that $H_S(s)$ can be approximated to an arbitrary accuracy by a stable rational transfer function.

The nonrational transfer function H_S forms the foundation of the controller parametrization. However, for easy inclusion of an integrator, for example, we also allow inclusion of a couple of arbitrary rational transfer functions, H_n, and define the set of controllers as follows

$$\left\{H_S(s)+\sum_{n=1}^{N_{PAR}}\varphi_n H_n(s)\,\middle|\,\boldsymbol{\rho}=\boldsymbol{K}\boldsymbol{x},\boldsymbol{x}\in\mathbb{R}^N\right\} \quad (15)$$

where $\boldsymbol{\rho}$ is a vector containing all ϕ_n and φ_n and $\boldsymbol{K}$ is a user defined real valued connection matrix. It can be used, for example, to force conjugate symmetry for the frequency response.

Evaluation of H_S in the complex plane is hard. However, the synthesis will be done entirely using the frequency response function. The frequency response of the controller is of the form $C(i\omega)=\boldsymbol{Y}(\omega)\boldsymbol{x}$, where $\boldsymbol{Y}$ is a complex valued row vector, whose elements can be evaluated using (11), (12), (13) and (15). Before implementing the controller a rational transfer function must be fitted to the frequency response function. This is shortly discussed in Section IV.

The parametrization is made applicable to discrete time systems using bilinear transformation which maps the left half of the s-plane to the interior of the unit circle in the z-plane, $z=(1+sT/2)/(1-sT/2)$, where T is the sampling period.

IV. EXAMPLE

In this section one way of performing smooth frequency domain parametric optimization is outlined using simple AMB control case as an example.

A. Process

Let us consider levitation of non rotating rigid rotor in magnetic bearings. The transfer function from control current reference to displacement is [18], [23]:

$$\boldsymbol{P}(s)=\boldsymbol{B}_s^{\mathrm{T}}\left(\boldsymbol{M}s^2-\boldsymbol{B}_b c\boldsymbol{B}_b^{\mathrm{T}}\right)^{-1}\boldsymbol{B}_b h \quad (16)$$

where h=340000, c=1.6×10^6, $\boldsymbol{M}$=diag([94.9 8.56]), where diag means diagonal matrix, and

$$\boldsymbol{B}_s=\begin{bmatrix}1 & 1\\ 0.361 & -0.526\end{bmatrix},\ \boldsymbol{B}_b=\begin{bmatrix}1 & 1\\ 0.287 & -0.451\end{bmatrix}. \quad (17)$$

B. Problem statement

We set a performance specification for output sensitivity function, $\boldsymbol{S}=(\boldsymbol{I}+\boldsymbol{PC})^{-1}$. In addition, any design freedom is used to maximize noise rejection. Mathematically, the task is to design a stabilizing controller, $\boldsymbol{C}(s)$, such that

$$\begin{aligned}\bar{\sigma}\left(W_S(\omega)\boldsymbol{S}(i\omega)\right)\le 1\ \forall\omega\in\psi_S\ \text{ and}\\ \bar{\sigma}\left(W_{CS}(\omega)\boldsymbol{C}(i\omega)\boldsymbol{S}(i\omega)/B\right)\le 1\ \forall\omega\in\psi_{CS},\end{aligned} \quad (18)$$

where B is "bound parameter", which we attempt to minimize and ψ_S and ψ_{CS} are the frequency regions where the specification must hold. In the present example, sensitivity weight, W_S, is 2 below 200 rad/s, 0.5 above 400 rad/s and changes linearly between the mentioned frequencies. $W_{CS}(\omega)=\max(0.2,(\omega/\omega_{CS})^2)$, where ω_{CS}=3000 rad/s. Frequency regions are ψ_S=[0,4000] rad/s and ψ_{CS}=[0,15000] rad/s.

In the present case we search the best decentralized stable

controller having identical diagonal entries, i.e. a controller of the form $\boldsymbol{C}(s)=\mathrm{diag}([C(s)\ C(s)])$. The problem statement is

$$\text{minimize } B \text{ subject to (18) and } \boldsymbol{C} \in \boldsymbol{F}, \tag{19}$$

where $\boldsymbol{F}$ is the set of proper controllers, which give stable closed loop and fulfill the defined structural constraints.

C. Controller parametrization

The controller grid was selected as $\psi_C=\{-10000, -9900,..., 10000\}$ rad/s. Because our present process has real valued input and output signals, the controller must exhibit conjugate symmetry. Thus, the free variable vector, $\boldsymbol{x}$, defines the imaginary part at nodes $\{100, 200,..., 9900\}$ rad/s, i.e. a total of 99 free variables. At negative frequencies the imaginary part is the opposite number, and at zero frequency, the imaginary part is zero. The roll-off rate of the Hilbert part in the symmetric case is 40 dB/dec, which is the same as the roll off rate set by the specifications (W_C).

D. The finite problem

With the parameterized controller the problem is now transformed to semi-infinite problem. Next, the problem is further reduced to finite problem by requiring that the specifications (18) are fulfilled in finite frequency grid, ψ_{CG}, called constraint grid. In the present case, due to the conjugate symmetry, it suffices to set the specifications for positive frequencies only. It is important that the constraint grid is sufficiently wide and dense compared to the controller grid and frequency behavior of the process so that violations of the constraints (18) outside the grid points remain in an acceptable level. The constraint grid was selected as $\psi_{CG}=\{40, 80,..., 12000\}$ rad/s.

In addition to creating frequency domain grids, the approximation of the largest singular value is introduced in this step. Constraints (18) are translated to

$$\begin{aligned} \eta\left(W_S(\omega)\boldsymbol{S}(i\omega)\right) &\le 1 \quad \forall \omega \in \psi_S \cap \psi_{CG} \\ \eta\left(W_C(\omega)C(i\omega)\boldsymbol{S}(i\omega)/B\right) &\le 1 \quad \forall \omega \in \psi_{CS} \cap \psi_{CG} \end{aligned} \tag{20}$$

Using equations of Sections II and III these constraints are transformed to form $\boldsymbol{g}(\boldsymbol{x},B)\le\boldsymbol{0}$, where $\boldsymbol{g}$ is vector valued function, which is twice continuously differentiable with respect to relevant argument values. The finite problem can be expressed in the form

$$\text{minimize } B \text{ subject to } \boldsymbol{g}(\boldsymbol{x},B) \le \boldsymbol{0} \text{ and } \boldsymbol{x} \in \boldsymbol{X}, \tag{21}$$

where $\boldsymbol{X}$ is the set of decision variable vectors, which gives stable closed loop. Note that the requirement of stable diagonal controller has been already embedded in $\boldsymbol{g}$. In the present case intersection $\psi_S \cap \psi_{CG}$ contains 100 frequency points and intersection $\psi_{KS} \cap \psi_{CG}$ contains 300 frequency points. So, $\boldsymbol{g}$ has a total of 400 elements.

E. Initial value and stability

In the present example we take care of constraint $\boldsymbol{x}\in\boldsymbol{X}$ by selecting an initial $\boldsymbol{x}_0\in\boldsymbol{X}$ and then ignoring constraint $\boldsymbol{x}\in\boldsymbol{X}$. In the present case this approach is justified because it is easy to find $\boldsymbol{x}_0\in\boldsymbol{X}$ and the constraint are such that near the boundaries of $\boldsymbol{X}$ some element of $\boldsymbol{g}$ should get high values, thus keeping the iterations inside $\boldsymbol{X}$. Of course, prerequisite for this is that the constraint grid is sufficiently dense. The initial controller was designed using manual loop-shaping:

$$C_{init}(s) = \frac{(0.05s+20)\omega_{init}^3}{(s+\omega_{init})\left(s^2+1.42\omega_{init}s+\omega_{init}^2\right)}, \tag{22}$$

where ω_{init}=2500 rad/2. The initial controller vector, $\boldsymbol{x}_0$, was fitted to C_{init} using least squares fit in the constraint frequency grid.

F. Optimization

Before going to actual optimization, we find a feasible solution, i.e. $\boldsymbol{x}\in\boldsymbol{X}$, which fulfills $\boldsymbol{g}(\boldsymbol{x},B_{max})\le\boldsymbol{0}$ for the maximum acceptable value of the bound parameter, B_{max}. This is done by solving

$$\text{minimize } A \text{ subject to } \boldsymbol{g}(\boldsymbol{x},B_{max}) \le A\boldsymbol{a}. \tag{23}$$

where $\boldsymbol{a}=\max(\boldsymbol{g}(\boldsymbol{x}_0,B_{max}),0)$. Iteration is started from $\boldsymbol{x}=\boldsymbol{x}_0$, A=1. This minimization can be terminated when $A\le 0$ is found. Problem (23) is a standard smooth constrained optimization problem, where tens of powerful methods are available [5], [21]. We have selected successive quadratic programming (SQP) as the algorithm category mainly because of good reputation of those algorithms and existing effective implementations. Many SQP implementations are able to guarantee global convergence to a Karush-Kuhn-Tucker point [17] and fast local convergence under realistic assumptions, [21]. We used the SQP algorithm in Matlab® Optimization Toolbox. Gradient information was provided for the algorithm according to (8).

Next, the optimization was performed, i.e. the problem

$$\text{minimize } B \text{ subject to } \boldsymbol{g}(\boldsymbol{x},B) \le \boldsymbol{0} \tag{24}$$

was solved using the same algorithm as in the feasibility stage. After 10 iterations, the algorithm converged to a final solution with B=222.7. The algorithm was terminated when the first order optimality conditions were fulfilled with sufficient tolerance. During the last iterations superlinear convergence was observed and the KKT point was certainly obtained.

The resulting controller, the sensitivity function and the disturbance rejection function are shown in Fig. 5. Those curves were computed with 1 rad/s grid to reveal any violations of the constraints also between the constraint frequency grid points. As can be seen, the constraints are violated only by a negligible amount. Another observation is that the boundaries are hit practically everywhere, which implies that the design cannot be considerably improved by increasing density of the grids.

G. Fitting of rational transfer function

A rational transfer function, C_{fit}, of order 9 was fitted to the obtained frequency response using the combination of algorithms found in [20] and [8], i.e. algorithm in the Matlab® Signal Processing Toolbox. It is also shown in Fig. 5 but it is not distinguishable from the original curve.

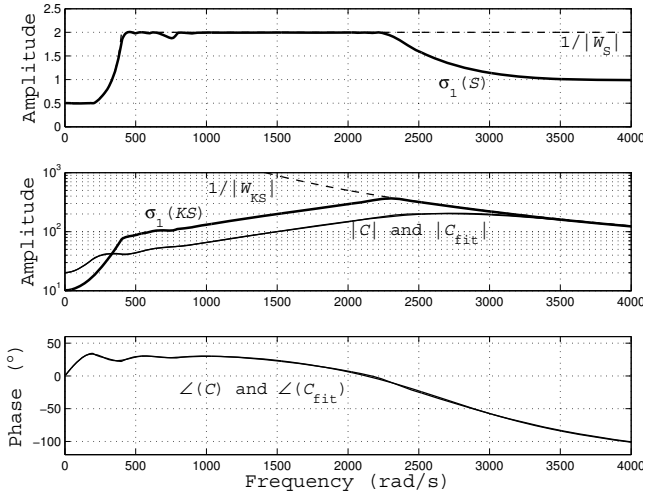

Fig 5. Results of the optimization.

V. CONCLUSIONS

It is clear that the method can handle multimodel uncertainties and multiple specifications without problems. The method extends also to structured singular value optimization in a straightforward way. The D-scales can be parametrized and the decision variable vector consisting of the controller parameters and D-scale parameters can be solved simultaneously as proposed in [3], but now using smooth optimization methods. As noted in [3], such approach has potential benefits compared to D-K iteration. Note that in the formulation outlined in Section IV we did not assume an explicit transfer function or state space model for the plant or the weights. This leads to difficulties in guaranteeing closed loop stability, but on the other hand, facilitates flexible definition of the specifications and also bringing measured frequency response data to synthesis process directly without model identification. So far we have successfully used frequency domain parametric optimization in several challenging industrial AMB applications.

REFERENCES

[1] H. Akcay, B. Ninness, "Othonormal basis functions for modeling continuous-time systems," *Signal Processing*, vol. 77, pp. 261-274, 1999.

[2] P. Apkarian, D. Noll, "Nonsmooth H_∞ Synthesis," *IEEE Transactions on Automatic Control*, vol. 51 no. 1, pp 71-86, 2006.

[3] P. Apkarian, H. Tuan, "Nonsmooth μ Synthesis," in *Proc. 11th Int. Conf. Control, Automation, Robotics and Vision.* Singapore, 7-10th December. pp. 917-922, 2010.

[4] G. Arfken, *Mathematical Methods for Physicists*. Academic Press Inc. Third edition, 1985.

[5] M. S. Bazaraa, H. D. Sherali, C. M. Shetty, *Nonlinear Programming, Theory and Algorithms*. Third Edition. John Wiley & Sons, Inc. 2006.

[6] H. W. Bode, *Network Analysis and Feedback Amplifier Design*. D. Van Nostrand Company Inc. USA. 1945.

[7] G. F. Bryant, G. D. Halikias, "Optimal loop-shaping for systems with large parameter uncertainty via linear programming," *International Journal of Control*, vol. 62, No. 3. pp. 557-568, 1995.

[8] J. Dennis, R. Schnabel, R. *Numerical Methods for Unconstrained Optimization and Nonlinear Equations*. Englewood Cliffs, NJ: Prentice Hall, 1983.

[9] R. Fittro, C. Knospe, "Rotor Compliance Minimization Via μ-Control of Active Magnetic Bearings," *IEEE Transactions on Control Systems Technology*, vol. 10, No. 2. pp. 238-249, 2002.

[10] C. Fransson, T. Wik, B. Lennartson, M. Saunders, P. Gutman, " Nonconservative Robust Control: Optimized and Constrained Sensitivity Functions," *IEEE Transactions on Control Systems Technology*, vol. 17, No. 2. pp. 298-308, 2009.

[11] A. Gera, I. Horowitz, "Optimization of the loop transfer function," *International Journal of Control*, vol. 31, No. 2, pp. 389-398, 1980.

[12] R. Greene, S. Kranz, *Function Theory of One Complex Variable*. Third edition. American Mathematical Society, 2006.

[13] E. A. Guillemin, *Synthesis of Passive Networks*. Jonh Wiley & Sons, Inc. 1957.

[14] I. M. Horowitz, *Synthesis of Feedback Systems*. Academic Press Inc. 1963.

[15] A. Karimi, G. Galdos, "Fixed-order H_∞ controller design for nonparametric models by convex optimization," *Automatica*, 46, pp. 1388-1394, 2010.

[16] T. Kato, *Perturbation theory for linear operators*. Springer-Verlag, 1966.

[17] H. W. Kuhn, A. W. Tucker, "Nonlinear Programming," *Proc. Second Berkeley Symposium on Mathematical Statistics and Probability*. University of California Press, Berkeley, 1951.

[18] E. Lantto, "Robust Control of Magnetic Bearings in Subcritical Machines," Ph.D. dissertation, *Acta Polytechnical Scandinavica*, Electrical Engineering Series 94, 143 p. Available: http://lib.tkk.fi/Diss/199X/isbn9512255758/, 1999.

[19] E. Lantto, J. Tommila, "A Supercritical 250 kW Industrial Air Compressor Prototype," *Journal of System Design and Dynamic,. Special issue on ISMB11,* vol. 3. No. 4. pp. 639-650. Available: http://www.jstage.jst.go.jp/article/ jsdd/3/4/3_639, 2009.

[20] E. Levi, "Complex Curve Fitting," *IRE Trans. on Automatic Control,* vol. AC-4, 1959.

[21] J. Nocedal, S. Wright, *Numerical Optimization*. Second Edition, Springer. 2006.

[22] K. B. Petersen, M. S. Pedersen, *The Matrix Cookbook*, http://matrixcookbook.com, 2008.

[23] G. Schweitzer, E. H. Maslen, *Magnetic Bearings, Theory, Design, and Application to Rotating Machinery*. Springer, 2009.

[24] U. Schönhoff, J. Luo, G. Li, E. Hilton, R. Nordman, P. Allaire, "Implementation of μ-synthesis Control for an Energy Storage Flywheel Test Rig," in *Proc. Seventh International Symposium on Magnetic Bearings*, Zurich, Switcherland. pp. 317-322, 2000.

[25] V. Zakian, U. Ak-Naib, "Design of dynamical and control systems by the method of inequalities," *Proceedings of the Institution of Electrical Engineers*, 120, 1421-1427, 1973.